sacrificed after 14 d. The length of the re-endothelialized area was significantly longer in binding HGF-treated rats than in control or HGF-treated rats. Neointimal formation was significantly greater in binding HGF-treated rats than in others.

In tissue engineering, design of scaffold has been the main target. Growth factors are usually physically mixed for utilization. However, to effectively utilize the growth factors, modification is favored. Covalent or noncovalent immobilization regulates the diffusion of growth factors to maintain the effects and provide specific microenvironments to regulate cellular responses with matrices.[146–150] In addition, the immobilization of growth factor is important for geometrical control of complex tissue formation of different types of cells within or near the scaffolds.

6. Future perspective

The field of tissue engineering has created a need for biomaterials that are capable of providing biofunctional and structural support for living cells outside the body. Most of the commonly used biomaterials in tissue engineering are designed based on their physico-chemical properties, thus achieving precise control over mechanical strength, compliance, porosity, and degradation kinetics. Biofunctional signals are added to the scaffold by tethering, immobilizing, or supplementing biofunctional macromolecules, such as growth factors, directly to the scaffold material. The challenge in tissue engineering remains to find the correct balance between the biofunctional and the physical properties of the scaffold materials for each application.[151] Communication between cells and extracellular environment using the engineered scaffold should be correctly regulated. For this purpose the surface biolization by immobilization of growth factor is a powerful tool for constructing elaborate intelligent biofuntional materials. Control of surface function with the immobilization is important for design. It will be also important to prepare biomaterials mimicking the growth factor proteins for mass production of biofunctional materials without using the native proteins.

References

1 Y. Ikada, *Tissue Engineering: Fundamentals and Applications*, Elsevier, Oxford, UK, 2006.
2 G. J. M. Cabrita, B. S. Ferreira, C. L. da Silva, R. Concalves, G. Almeida-Porada and J. M. S. Cabral, *Trends Biotechnol.*, 2003, **21**, 233–240.
3 N. Panoskaltsis, A. Mantalaris and J. H. D. Wu, *J. Biosci. Bioeng.*, 2005, **100**, 28–35.
4 D. Marolt, A. Augst, L. E. Freed, C. Vepari, R. Fajardo, N. Patel, M. Gray, M. Farley, D. Kaplan and G. Vunjak-Novakovic, *Biomaterials*, 2006, **27**, 6138–6149.
5 Y. Ito, H. Hasuda, T. Kitajima and T. Kiyono, *J. Biosci. Bioeng.*, 2006, **102**, 467–469.
6 Y. Ito, M. Kawamorita, T. Yamabe, T. Kiyono and K. Miyamoto, *J. Biosci. Bioeng.*, 2007, **103**, 113–121.
7 Y. Hirano and D. J. Mooney, *Adv. Mater.*, 2004, **16**, 17–25.
8 J. Spatz, *Soft Matter*, 2007, **3**, 261–262.
9 P. Cuatrecasas, *Proc. Natl. Acad. Sci. U. S. A.*, 1969, **63**, 450–457.
10 R. W. Butcher, O. B. Croffird, S. Gammeltoff, J. Gilemann, J. R. Gavin, J. D. Goldfine, C. R. Kahn, M. Rodbell, J. Roth, L. Jarett, R. J. Lefkowitz, R. Levine and G. V. Marinetti, *Science*, 1973, **182**, 396–397.
11 T. Oka and Y. Topper, *Proc. Natl. Acad. Sci. U. S. A.*, 1974, **71**, 1630–1633.
12 H. J. Kolb, R. Renner, K. D. Weiss and O. H. Wieland, *Proc. Natl. Acad. Sci. U. S. A.*, 1975, **72**, 248–252.
13 P. Cuatrecasas, *Science*, 1973, **182**, 397–398.
14 J. C. Venter, *Pharmacol. Rev.*, 1982, **34**, 153–257.
15 J. L. Garwin and T. D. Gelehter, *Arch. Biochem. Biophys.*, 1974, **164**, 52–59.
16 Y. Ito, S. Q. Liu and Y. Imanishi, *Biomaterials*, 1991, **12**, 449–453.
17 S. Q. Liu, Y. Ito and Y. Imanishi, *Biomaterials*, 1992, **13**, 50–58.
18 Y. Ito, S. Q. Liu, M. Nakabayashi and Y. Imanishi, *Biomaterials*, 1992, **13**, 789–794.
19 S. Q. Liu, Y. Ito and Y. Imanishi, *J. Biochem. Biophys. Methods*, 1992, **25**, 139–148.
20 S. Q. Liu, Y. Ito and Y. Imanishi, *Enzyme Microb. Technol.*, 1993, **15**, 167–172.
21 Y. Ito, J. Zheng, Y. Imanishi, K. Yonezawa and M. Kasuga, *Proc. Natl. Acad. Sci. U. S. A.*, 1996, **93**, 3598–3601.
22 Y. Ito, T. Uno, S. Q. Liu and Y. Imanishi, *Biotechnol. Bioeng.*, 1992, **40**, 1271–1276.
23 S. Q. Liu, Y. Ito and Y. Imanishi, *J. Biomed. Mater. Res.*, 1993, **27**, 909–915.
24 Y. Ito, S. Q. Liu, T. Orihara and Y. Imanishi, *J. Bioact. Compat. Polym.*, 1994, **9**, 170–183.
25 I. K. Kang, S.-H. Choi, D.-S. Shin and S. C. Yoon, *Int. J. Biol. Macromol.*, 2001, **28**, 205–212.
26 Y. Ito, M. Inoue, S. Q. Liu and Y. Imanishi, *J. Biomed. Mater. Res.*, 1993, **27**, 901–907.
27 G. Chen, Y. Ito and Y. Imanishi, *Bioconjugate Chem.*, 1997, **8**, 106–110.
28 L. Bromberg and L. Salvati, Jr., *Bioconjugate Chem.*, 1999, **10**, 678–686.
29 E. J. Kim, I. K. Kang, M. K. Jang and Y. B. Park, *Biomaterials*, 1998, **19**, 239–249.
30 J. Tessmar, A. Mikos and A. Gopferich, *Biomaterials*, 2003, **24**, 4475–4486.
31 K. Kellner, J. Tessmar, S. Milz, P. Angele, M. Nerlich, M. B. Schulz, T. Blunk and A. Gopferich, *Tissue Eng.*, 2004, **10**, 429–440.
32 J. Tessmar, K. Kellner, M. B. Schulz, T. Blunk and A. Gopferich, *Tissue Eng.*, 2004, **10**, 441–453.
33 J. Zheng, Y. Ito and Y. Imanishi, *Biomaterials*, 1994, **15**, 963–968.
34 Y. Ito, J. Zheng and Y. Imanishi, *Biotechnol. Bioeng.*, 1995, **45**, 144–148.
35 J. Zheng, Y. Ito and Y. Imanishi, *J. Biomater. Sci., Polym. Ed.*, 1995, **7**, 515–522.
36 J. Zheng, Y. Ito and Y. Imanishi, *Biotechnol. Prog.*, 1995, **11**, 677–681.
37 J.-S. Li, Y. Ito, J. Zheng, T. Takahashi and Y. Imanishi, *J. Biomed. Mater. Res.*, 1997, **31**, 190–197.
38 Y. Ito, J. Zheng and Y. Imanishi, *Biomaterials*, 1997, **18**, 197–202.
39 M. Gumusdrelioglu and H. Turkoglu, *Biomaterials*, 2002, **23**, 3927–3935.
40 M. Gumusdrelioglu and A. G. Karakecili, *J. Biomater. Sci., Polym. Ed.*, 2003, **14**, 199–211.
41 Y. J. Kim, I. K. Kang, M. W. Huh and S. C. Yoon, *Biomaterials*, 2000, **21**, 121–130.
42 Y. Ito, G. Chen and Y. Imanishi, *Biotechnol. Prog.*, 1996, **12**, 700–703.
43 Y. Ito, S. Kondo, G. Chen and Y. Imanishi, *FEBS Lett.*, 1997, **403**, 159–162.
44 G. Chen, Y. Ito and Y. Imanishi, *Biotechnol. Bioeng.*, 1997, **53**, 339–344.
45 H. Hatakeyama, A. Kikuchi, M. Yamato and T. Okano, *Biomaterials*, 2006, **27**, 5069–5078.
46 H. Hatakeyama, A. Kikuchi, M. Yamato and T. Okano, *Inflammation Regener.*, 2006, **26**, 437–445.
47 H. Hatakeyama, A. Kikuchi, M. Yamato and T. Okano, *Biomaterials*, 2007, **28**, 3632–3643.
48 P. R. Kuhl and L. G. Griffith-Cima, *Nat. Med.*, 1996, **2**, 1022–1027.
49 J. Ichinose, M. Morimatsu, T. Yanagida and Y. Sako, *Biomaterials*, 2006, **27**, 3343–3350.

50 M. Nakajima, T. Ishimuro, K. Kato, I.-K. Ko, I. Hirata, Y. Arima and H. Iwata, *Biomaterials*, 2007, **28**, 1048–1060.
51 Y. Ito, J.-S. Li, T. Takahashi, Y. Imanishi, Y. Okabayashi, Y. Kido and M. Kasuga, *J. Biochem.*, 1997, **121**, 514–520.
52 B. J. Klenkler, M. Griffith, C. Becerril, J. A. West-Mays and H. Sheardown, *Biomaterials*, 2005, **26**, 7286–7296.
53 B. J. Klenkler and H. Sheardown, *Biotechnol. Bioeng.*, 2006, **95**, 1158–1166.
54 G. Chen, Y. Ito and Y. Imanishi, *Biochim. Biophys. Acta*, 1997, **1358**, 200–208.
55 Y. Ito, G. Chen and Y. Imanishi, *Bioconjugate Chem.*, 1998, **9**, 277–282.
56 G. Chen, Y. Ito, S. Masuda and R. Sasaki, *Cytotechnology*, 2001, **35**, 3–8.
57 G. Chen and Y. Ito, *Biomaterials*, 2001, **22**, 2453–2457.
58 Y. Ito, G. Chen, Y. Imanishi, T. Morooka, E. Nishida, Y. Okabayashi and M. Kasuga, *J. Biochem.*, 2001, **129**, 733–737.
59 Y. K. Woo, S. Y. Kwon, H. S. Lee and Y. S. Park, *J. Orthop. Res.*, 2007, **25**, 73–80.
60 N. Nishi, O. Matsushita, K. Yuube, H. Miyanaka, A. Okabe and F. Wada, *Proc. Natl. Acad. Sci. U. S. A.*, 1998, **95**, 7018–7023.
61 M. Hayashi, M. Tomita and K. Yoshizato, *Biochim. Biophys. Acta*, 2001, **1528**, 187–195.
62 T. Ishikawa, H. Terai and T. Kitajima, *J. Biochem.*, 2001, **129**, 627–633.
63 K. Ogiwara, M. Nagaoka, C.-S. Cho and T. Akaike, *Biotechnol. Lett.*, 2005, **27**, 1633–1637.
64 K. Ogiwara, M. Nagaoka, C.-S. Cho and T. Akaike, *Biochem. Biophys. Res. Commun.*, 2006, **345**, 255–259.
65 I. Elloumi, R. Kobayashi, H. Funabashi, M. Mie and E. Kobatake, *Biomaterials*, 2006, **27**, 3451–3458.
66 T. Nakaji-Hirabayashi, K. Kato, Y. Arima and H. Iwata, *Biomaterials*, 2007, **28**, 357–3529.
67 S. C. Shibata, K. Hibino, T. Mashimo, T. Yanagida and Y. Sako, *Biochem. Biophys. Res. Commun.*, 2006, **342**, 316–322.
68 T. A. Kapur and M. S. Schoichet, *J. Biomater. Sci., Polym. Ed.*, 2003, **14**, 383–394.
69 T. A. Kapur and M. S. Schoichet, *J. Biomed. Mater. Res.*, 2004, **68A**, 235–243.
70 P. R. Chen, M. H. Chen, F. H. Lin and W. Y. Su, *Biomaterials*, 2005, **26**, 6579–6587.
71 Y. Ito, *Jpn. J. Artif. Organs*, 1998, **27**, 383–394.
72 N. Gomez, Y. Lu, S. Chen and C. E. Schmidt, *Biomaterials*, 2007, **28**, 271–284.
73 D. A. Puleo, R. A. Kissling and M. S. Sheu, *Biomaterials*, 2002, **23**, 2079–2087.
74 H. Schliphake, A. Aref, D. Scharnweber, S. Bierbaum, S. Roessler and A. Sewing, *Clin. Oral Impl. Res.*, 2005, **16**, 563–569.
75 H. Tsujigiwa, H. Nagatsuka, M. Gunduz, A. Rodriguez, A. J. Rivera, R. Z. Legeros, M. Inoue and N. Nagai, *J. Biomed. Mater. Res.*, 2005, **75**, 210–215.
76 H. Tsujigiwa, H. Nagatsuka, Y. J. Lee, P. P. Han, M. Gunduz, R. Z. LeGeros, M. Inoue, M. Yamada and N. Nagai, *J. Biomed. Mater. Res.*, 2006, **77A**, 507–511.
77 Y. J. Park, K. H. Kim, J. Y. Lee, Y. Ku, S. J. Lee, B. M. Min and C. P. Chung, *Biotechnol. Appl. Biochem.*, 2006, **43**, 17–24.
78 H.-W. Liu, C.-H. Chen, C.-L. Tsai, I-H. Lin and G.-H. Hsiue, *Tissue Eng.*, 2007, **13**, 1113–1124.
79 T. Taguchi, A. Kishida and M. Akashi, *J. Bioact. Compat. Polym.*, 2000, **15**, 309–320.
80 Y. Ito, H. Hasuda, H. Terada and T. Kitajima, *J. Biomed. Mater. Res.*, 2005, **74**, 659–665.
81 M. V. Backer, V. Patel, B. T. Jehning, K. P. Claffey and J. M. Backer, *Biomaterials*, 2006, **27**, 5452–5458.
82 K. Watanabe, T. Miyazaki and R. Matsuda, *Zool. Sci.*, 2003, **20**, 429–434.
83 S. Inoue and Y. Tabata, *Inflammation Regener.*, 2006, **26**, 181–184.
84 Y. Ito, M. Hayashi and Y. Imanishi, *J. Biomater. Sci., Polym. Ed.*, 2001, **12**, 367–378.
85 T. Ohyama, T. Nishide, H. Iwata, H. Sato, M. Toda, N. Toma and W. Taki, *J. Neurosurg.*, 2005, **102**, 109–115.
86 U. Fischer, U. Hempel, D. Becker, S. Bierbaum, D. Scharnweber, H. Worch and K. W. Wenzel, *Biomaterials*, 2003, **24**, 2631–2641.
87 K. Merret, C. M. Griffith, Y. Deslandes, G. Pleizier, M. A. Dube and H. Sherwood, *J. Biomed. Mater. Res.*, 2003, **67A**, 981–993.
88 C.-H. Chou, W. T. K. Cheng, C.-C. Lin, C.-H. Chang, C.-C. Tsai and F.-H. Lin, *J. Biomed. Mater. Res.*, 2006, **77B**, 338–348.
89 B. K. Mann, R. H. Schmedlen and J. L. West, *Biomaterials*, 2001, **22**, 439–444.
90 T. Kitajima, H. Terai and Y. Ito, *Biomaterials*, 2007, **28**, 1989–1997.
91 N. Ohkawara, H. Ueda, S. Shinozaki, T. Kitajima, Y. Ito, H. Asaoka, A. Kawakami, E. Kaneko and K. Shimokado, *J. Atheroscler. Thromb.*, 2007, **14**, 185–191.
92 T. Konno, S. Sakano, S. Higashida and Y. Ito, *Inflammation Regener.*, 2005, **25**, 426–430.
93 B. Varnum-Finney, L. Wu, M. Yu, C. Brashem-Stain, S. Staats, D. Flowers, J. D. Griffin and I. D. Bernstain, *J. Cell Sci.*, 2000, **113**, 4313–4318.
94 L. Vas V. Szilagyi, K. Paloczi and F. Uher, *J. Leukocyte Biol.*, 2004, **75**, 714–720.
95 B. L. Beckstead, D. M. Santosa and C. M. Giachelli, *J. Biomed. Mater. Res.*, 2006, **79A**, 94–103.
96 H. Makino, H. Hasuda and Y. Ito, *J. Biosci. Bioeng.*, 2004, **98**, 374–379.
97 G. Cetinkaya, H. Torkoglu, S. Arat, H. Odaman, M. A. Onur, M. Gumusderelioglu and A. Tumer, *J. Biomed. Mater. Res.*, 2007, **81A**, 911–919.
98 J. G. Doheny, E. J. Jervis, M. M. Guarna, R. K. Humphries, R. A. J. Warren and D. G. Kilburn, *Biochem. J.*, 1999, **339**, 429–434.
99 J. I. Horwitz, M. Toner, R. G. Tompkins and M. J. Yarmush, *Mol. Immunol.*, 1993, **30**, 1041–1048.
100 D. H. Kim, J. T. Smith, A. Chilkoti and W. M. Reichert, *Biomaterials*, 2007, **28**, 3369–3377.
101 Y. Guan, H. Zhong, X. Wang and T. Zhou, *Shengwu Yixue Gongchengxue Zazhi*, 2006, **23**, 346–349.
102 Y. Ito, H. Hasuda, T. Yamauchi, N. Komatsu and K. Ikebuchi, *Biomaterials*, 2004, **25**, 2293–2298.
103 S. Q. Liu, Y. Ito and Y. Imanishi, *Int. J. Biol. Macromol.*, 1993, **15**, 221–226.
104 M. Nagaoka, U. Koshimizu, S. Yuasa, F. Hattori, H. Chen, T. Tanaka, M. Okabe, K. Fukuda and T. Akaike, *PLoS ONE*, 2006, **e15**, 1–7.
105 S. M. Martin, R. Ganapathy, T. K. Kim, D. Leach-Scampavia, C. M. Giachelli and B. D. Ratner, *J. Biomed. Mater. Res.*, 2003, **67A**, 334–343.
106 S. M. Martin, J. L. Schwartz, C. M. Giachelli and B. D. Ratner, *J. Biomed. Mater. Res.*, 2004, **70A**, 10–19.
107 J. Koike, K. Nagata, S. Kudo, T. Tsuji and T. Irimura, *FEBS Lett.*, 2000, **477**, 84–88.
108 N. Kohrgruber, M. Groger, P. Meraner, E. Kriehuber, P. Petzelbauer, S. Brandt, G. Stingl, A. Rot and D. Maurer, *J. Immunol.*, 2004, **173**, 6592–6602.
109 J. E. Ho, E. H. Chung, S. Wall, D. V. Shaffer and K. E. Healy, *J. Biomed. Mater. Res.*, 2007, DOI: 10.1002/jbm.a.31355.
110 J. Massague and A. Pandiella, *Annu. Rev. Biochem.*, 1993, **62**, 515–541.
111 R. Iwamoto and E. Mekada, *Cytokine Growth Factor Rev.*, 2000, **11**, 335–344.
112 Y. Ito, G. Chen and Y. Imanishi, *J. Biomater. Sci., Polym. Ed.*, 1998, **9**, 879–890.
113 S. Drotleft, U. Lungwitz, M. Breunig, A. Dennis, T. Blunk, J. Tessmar and A. Gopferich, *Eur. J. Pharm. Biopharm.*, 2004, **58**, 385–407.
114 Y. Ito and M. Nogawa, *Biomaterials*, 2003, **24**, 3021–3026.
115 Y. Ito, *Biotechnol. Prog.*, 2006, **22**, 924–932.
116 R. Weissleder, K. Kelly, E. Y. Sun, T. Shtatland and L. Josephson, *Nat. Biotchnol.*, 2005, **23**, 1418–1423.
117 L. L. Kiessling, J. E. Gestwicki and L. E. Strong, *Angew. Chem., Int. Ed.*, 2006, **45**, 2348–2368.
118 S. Sasagawa, Y. Ozaki, K. Fujita and S. Kuroda, *Nat. Cell Biol.*, 2005, **7**, 365–373.
119 C. C. Reddy, S. K. Niyogi, A. Wells, H. S. Wiley and D. A. Lauffenburger, *Nat. Biotechnol.*, 1996, **14**, 1696–1699.
120 Y. Ito, *Biomaterials*, 1999, **20**, 2333–2342.
121 U. Schwarz, *Soft Matter*, 2007, **3**, 263–266.

122 I. Levental, P. C. Georges and P. A. Janmey, *Soft Matter*, 2007, **3**, 299–306.
123 P. P. Girard, E. A. Cavalcanti-Adam, R. Kemkemer and J. P. Spatz, *Soft Matter*, 2007, **3**, 307–326.
124 D. Falconnet, G. Csucs, H. M. Gradin and M. Textor, *Biomaterials*, 2006, **27**, 3044–3063.
125 A. Khademhosseini, R. Langer, J. Borenstein and J. P. Vacanti, *Proc. Natl. Acad. Sci. U. S. A.*, 2006, **103**, 2480–2487.
126 W. F. Liu and C. S. Chen, *Mater. Today*, 2005, **8**, 28–35.
127 C. S. Chen, X. Jiang and G. M. Whitesides, *MRS Bull.*, 2005, **30**, 194–201.
128 T. Xu, J. Jin, C. Gregory, J. J. Hickman and T. Boland, *Biomaterials*, 2005, **26**, 93–99.
129 A. S. G. Curtis, *Eur. Cells Mater.*, 2004, **8**, 27–36.
130 T. H. Park and M. L. Shuler, *Biotechnol. Prog.*, 2003, **19**, 243–253.
131 D. R. Jung, R. Kapur, T. Adams, K. A. Giuliano, M. Mrksich, H. G. Craighead and D. L. Taylor, *Crit. Rev. Biotechnol.*, 2001, **21**, 111–154.
132 A. Folch and M. Toner, *Annu. Rev. Biomed. Eng.*, 2000, **2**, 227–256.
133 C. S. Chen, M. Mrksich, S. Huang, G. M. Whitesides and D. E. Ingber, *Science*, 1997, **276**, 1425–1428.
134 C. H. Thomas, J. H. Collier, C. S. Sfeir and K. E. Healy, *Proc. Natl. Acad. Sci. U. S. A.*, 2002, **99**, 1972–1977.
135 R. McBeath, D. M. Pirone, C. M. Nelson, K. Bhadriraju and C. S. Chen, *Dev. Biol.*, 2004, **6**, 483–495.
136 C. M. Nelson, R. P. Jean, J. L. Tan, W. F. Liu, N. J. Sniadecki, A. A. Spector and C. S. Chen, *Proc. Natl. Acad. Sci. U. S. A.*, 2005, **102**, 11594–11599.
137 S. N. Bhatia, U. M. L. Yarmush and M. Toner, *J. Biomed. Mater. Res.*, 1997, **34**, 189–199.
138 M. Yamato, C. Konno, M. Utsumi, A. Kikuchi and T. Okano, *Biomaterials*, 2002, **23**, 561–567.
139 A. Khademhosseini, K. Y. Suh, J. M. Yang, G. Eng, J. Yeh, S. Levenberg and R. Langer, *Biomaterials*, 2004, **25**, 3583–3359.
140 D. T. Chiu, N. L. Jeon, S. Huang, R. S. Kane, C. J. Wargo, I. S. Choi, D. E. Ingber and G. M. Whitesides, *Proc. Natl. Acad. Sci. U. S. A.*, 2000, **97**; 2408–2413.
141 M. D. Tang, A. P. Golden and J. Tien, *J. Am. Chem. Soc.*, 2003, **125**, 12988–12989.
142 Y. Ito, G. Chen, Y. Guan and Y. Imansihi, *Langmuir*, 1997, **13**, 2756–2759.
143 J. Nakanishi, Y. Kikuchi, T. Takarada, H. Nakayama, K. Yamaguchi and M. Maeda, *J. Am. Chem. Soc.*, 2004, **126**, 16314–16315.
144 J. Nakanishi, Y. Kikuchi, S. Inoue, K. Yamaguchi, T. Takarada and M. Maeda, *J. Am. Chem. Soc.*, 2007, **129**, 6694–6695.
145 J. Edahiro, K. Sumaru, Y. Tada, K. Ohi, T. Takagi, M. Kameda, T. Shinbo, T. Kanamori and Y. Yoshimi, *Biomacromolecules*, 2005, **6**, 970–974.
146 T. Boontheekul and D. J. Mooney, *Curr. Opin. Biotechnol.*, 2003, **14**, 559–565.
147 R. Vasita and D. S. Katti, *Expert Rev. Med. Devices*, 2006, **3**, 29–47.
148 M. P. Lutolf and J. A. Hubbell, *Nat. Biotechnol.*, 2005, **23**, 47–55.
149 H. J. Kong and D. J. Mooney, *Nat. Rev. Drug Discovery*, 2007, **6**, 455–463.
150 K. Saha, J. F. Pollock, D. V. Schaffer and K. Healy, *Curr. Opin. Chem. Biol.*, 2007, **11**, 381–387.
151 D. Seliktar, *Ann. N. Y. Acad. Sci.*, 2005, **1047**, 386–394.

eXPRESS Polymer Letters Vol.2, No.3 (2008) 165–183
Available online at www.expresspolymlett.com
DOI: 10.3144/expresspolymlett.2008.22

Stimuli-responsive poly(ampholyte)s containing L-histidine residues: synthesis and protonation thermodynamics of methacrylic polymers in the free and in the cross-linked gel forms

M. Casolaro[1], Y. Ito[2,3], T. Ishii[2], S. Bottari[4], F. Samperi[5], R. Mendichi[6]*

[1]Dipartimento di Scienze e Tecnologie Chimiche e dei Biosistemi, Via Aldo Moro 2, Università degli Studi di Siena, I-53100 Siena, Italy
[2]RIKEN (The Institute of Physical and Chemical Research), Hirosawa 2-1, Wako, Saitama 351-0198, Japan
[3]Kanagawa Academy of Science and Technology, KSP East 309, Sakado 3-2-1, Takatsu-ku, Kawasaki, Kanagawa 213-0012, Japan
[4]Dipartimento di Fisica, Via Roma, Università degli Studi di Siena, I-53100 Siena, Italy
[5]Istituto di Chimica e Tecnologia dei Polimeri – Sez. Catania (CNR) – Dipartimento di Chimica, Università di Catania, Viale A. Doria 6, I-95125 Catania, Italy
[6]Istituto per lo Studio delle Macromolecole (CNR), Via E. Bassini 15, I-20133 Milano, Italy

Received 12 November 2007; accepted in revised form 14 January 2008

Abstract. Methacrylate-structured poly(ampholyte)s were synthesized in the homopolymer and copolymer forms starting from the *N*-methacryloyl-L-histidine (MHist) and the *N*-isopropylacrylamide (NIPAAm). They were also obtained in the cross-linked (hydrogel) form, showing a close thermodynamic behaviour as that shown by the corresponding soluble free polymer analogues. Viscometric data revealed that the minimum hydrodynamic volume of the polymer at its isoelectric point (pH 5) shifted to lower pHs as the NIPAAm content increased, and beyond a critical low MHist content the reduced viscosity decreased, even at low pHs. The phenomenon was attributed to hydrophobic forces between the isopropyl groups outweighing the repulsive electrostatic interactions of the polymer in the positively charged form. A similar behaviour was shown by the corresponding hydrogel. The latter also revealed a different phase transition phenomenon induced by external stimuli (temperature, pH, ionic strength, electric current) when compared to the acrylate-structured analogues. The polyMHist, as well as the corresponding monomer, was found for two days to be non toxic against the mouse osteoblasts (MC3T3-E1).

Keywords: *biocompatible polymers, smart polymers, polymer gels, protonation thermodynamics, polyampholytes*

1. Introduction

Vinyl compounds carrying aminoacid residues have been widely synthesized to obtain functional polymers for practical purposes [1]. The presence of the carboxyl [2] or the amino [3] functionality made these polymers sensitive to the pH in a range that was closely related to their basicity constants. Moreover, the presence of the hydrophilic amido functionality and the hydrophobic isopropyl groups in the side chain made these polymers also sensitive to the temperature [4, 5].

Recently, new vinyl acrylate polymers based on the L-histidine residues have been developed in order to have poly(ampholyte)s responding in different pH-ranges [6]. The imidazole-containing methacrylate polymers with different functions were investi-

*Corresponding author, e-mail: casolaro@unisi.it

gated in the catalytic activities towards the solvolyses of a series of activated phenyl esters [7]. Besides the buffering capacity of proteins in the physiological pH range, the imidazole group is also able to form coordination compounds with metal ions [8]. These compounds are considered as models for the understanding of the biological activity of proteins involved in fatal disorders such as the Alzheimer's disease or the prion infection [9, 10]. Synthetic polymers containing the imidazole functionality have recently been reported as thermosensitive, reusable displacers for immobilized metal affinity chromatography of proteins [11, 12]. The incorporation of the imidazole functionality in the highly branched poly(*N*-isopropylacrylamide), the polyNIPAAm, showed interest as a thermally responsive 'smart' polymer for the purification of a histidine-tagged protein fragments [13, 14]. Moreover, the absence of toxicity makes these ampholyte polymers useful candidates in the development of loosely cross-linked hydrogels to be used as injectable polymer scaffolds for tissue engineering applications [15]. The non toxic effect of the poly(MHist) against the osteoblast cells enables the corresponding hydrogels to be tailored in medical treatment for more efficient routes in the administration of pharmaceutical compounds, especially metal-based drugs [16], and improves the absorption of loaded amino-bisphosphonates (BPs) in the bone resorption process [17, 18]. In the latter case, the poor absorption of bisphosphonates via the paracellular route may be improved by a slow releasing process of BPs loaded into the hydrogel.

Previous reported papers described the thermodynamic behaviour of acrylate polymers with the L-histidine residues in the free and in the cross-linked forms [6]. Copolymers with the *N*-isopropylacrylamide were also prepared to obtain multiple stimuli-sensitive hydrogels for biomedical applications [19, 20]. In fact, besides the pH, they were sensitive to the temperature, the electric potential, the salt-type and the ionic strength.

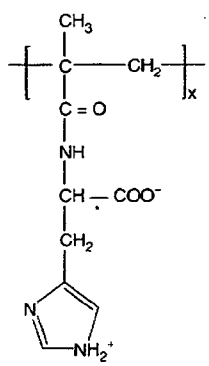

Figure 1. Structure of the monomer unit of poly(MHist)

Following our interest in these kind of polymers, we thought to study the methacrylate-structured polymer analogues because, as a rule, the solution behaviour of acrylate compounds differs to some extent from that of the corresponding methacrylate [21]. Thus, the aim of this paper is devoted to the protonation behaviour study of the synthetic methacrylic poly(ampholyte)s containing the L-histidine residues, the poly(MHist) (Figure 1).

A series of copolymers with a variable amount of NIPAAm was studied in order to clarify their thermodynamic behaviour in view of the potential applications of the corresponding hydrogels. The thermodynamic study of either the soluble or the cross-linked polymers allowed to evaluate the basicity constants along with the enthalpy and entropy changes during the protonation of the imidazole nitrogen. Moreover, the results of the swelling properties of three different cross-linked hydrogels were reported along with their protonation behaviour. They were strictly compared to the previously reported acrylate analogues [6, 19].

The hydrophilic behaviour of the non toxic poly (MHist) allowed the preparation of a new type of copolymer for nonbiofouling surfaces [22]. The polystyrene hydrophilization with poly(MHist) and some of its copolymers was in fact shown to be higher than that of the BSA (Bovine Serum Albumin).

2. Experimental section

2.1. Materials

L-Histidine (98%), methacryloyl chloride (97%) and 2,2'-azoisobutironitrile (AIBN, 98%) were purchased from Wako Pure Chemical Industries. Ammonium peroxo-disulfate (APS, 98%) and *N,N,N',N'*-tetramethylethylenediamine (TEMED) were from Kanto Chemical *Co.*, Inc. *N,N'*-ethylenebis-acrylamide (EBA, 98%) and triethylamine (TEA, 99.5%) were from Fluka *Co.* The AIBN was recrystallized from methanol and all the other reagents were used as received. The *N*-isopropylacrylamide (NIPAAm, Wako Co.) was purified by recrystallization from *n*-hexane and then dried in vacuo. Buffer solutions (tris, phosphate, acetate)

were prepared at a concentration of 0.01M in twice-distilled water and in 0.15M NaCl. The sodium chloride salt was of analytical grade from Fluka *Co.*

2.2. Syntheses

Synthesis of MHist

The *N*-methacryloyl-L-histidine, MHist, was prepared according to the previously reported synthetic routes [22, 24]. To an aqueous solution of L-histidine (5.0 g, 32 mmol) and sodium hydroxide (1.6 g, 40 mmol) in twice-distilled water (20 ml), the methacryloyl chloride (3.67 ml, 38 mmol), diluted in dioxane (10 ml), was added dropwise. During addition, the reaction mixture was kept under 5°C by the external ice-bath cooling, and then the temperature was raised to room temperature for 1 hour. After removing the dioxane by a rotary evaporator, the mixture was acidified to pH 2 with concentrated hydrochloric acid and extracted with ether. The aqueous layer was adjusted to pH 5 and concentrated in vacuo to obtain crude MHist. The crude monomer was purified by repeated precipitations from ethanol to acetone and dried in vacuo.

Synthesis of polyMHist

The poly(*N*-methacryloyl-L-histidine), polyMHist, was synthesized by a conventional free-radical polymerization [25]. The polymer was obtained as follows. A mixture of MHist (0.5 mmol) in ethanol (20 ml) containing AIBN (0.05 mmol) was purged with N_2 gas and then allowed to react under nitrogen atmosphere at 70°C for 20 h. The obtained polymer was purified by using a dialysis cellophane tubing-seamless (MWCO 3500 g/mol) in twice-distilled water for 2 days and then lyophilized to give a white powder.

Synthesis of poly(MHist-co-NIPAAm)

The poly(*N*-methacryloyl-L-histidine-*co*-*N*-isopropylacrylamide), poly(MHist-*co*-NIPAAm), copolymers were synthesized by the conventional free-radical polymerization reaction. Three different samples of the NIPAAm/MHist copolymers with decreasing amounts of MHist, namely co-3, co-2, and co-1, were synthesized. The mixture of MHist and NIPAAm with different molar ratio (the total mole was adjusted to 20 mmol) in twice-distilled water (40 ml), and containing 30 µl of TEMED 10 mM solution, was purged with N_2 gas and then 100 µl of APS 5 mM solution were added and allowed to react under nitrogen atmosphere at room temperature for 18 h. The polymer obtained was purified by using a dialysis cellophane tubing-seamless (MWCO 3500 g/mol) in twice-distilled water for 2 days and then lyophilized to give a white powder.

Synthesis of hydrogels

Three hydrogel samples containing only MHist (MH2) and a mixture of NIPAAm/MHist (CMH2, CMH10), were prepared according to a previously reported procedure [6, 19, 26]. The two poly (MHist-*co*-NIPAAm) hydrogels, at a NIPAAm/MHist molar ratio of 12, were synthesized by cross-linking with 2 (CMH2) and 10 (CMH10) mol% of EBA. The hydrogel MH2 was obtained only with the MHist cross-linked with 2 mol% of EBA. The synthesis was carried out in a glass tube, containing the monomer solution at a total concentration of 15 wt%, after their degassing under vacuum and under a nitrogen atmosphere. The reaction mixture was kept at room temperature for 24 h even if the gelation was observed within 4 h. Afterwards, the gel samples were removed, thoroughly washed with twice-distilled water for two weeks, and then slowly dried at r.t. to a constant weight. In all cases, the yield was more than 90%.

2.3. Spectroscopic and molecular characterization

The molecular characterization of polyMHist homopolymer and related copolymers was performed by a multi-angle laser light scattering (MALS) Dawn DSP-F photometer from Wyatt (Santa Barbara, CA, USA) on-line to a size exclusion chromatography (SEC) system. The SEC-MALS experimental conditions were the following: 0.2M NaCl + 0.1M Tris buffer pH 8.0 as mobile phase, two TSKgel PW G4000 and G3000 columns from Tosoh Bioscience (Stuttgart, D), 35°C of temperature, 0.8 ml/min of flow rate and 150 µl of injection volume. The wavelength of the MALS He-Ne laser was 632.8 nm. The light scattering signal was simultaneously detected at fifteen

scattering angles ranging in the solvent from 14.5° to 151.3°. The calibration constant was calculated using toluene as standard assuming a Rayleigh Factor of $1.406 \cdot 10^{-5}$ cm^{-1}. The angular normalization was performed by measuring the scattering intensity of a concentrated solution of a BSA globular protein in the mobile phase assumed to act as an isotropic scatterer. The refractive index increment, dn/dc, of polyMHist homopolymer and copolymers with respect to the used solvent was measured by a KMX-16 differential refractometer from LDC Milton Roy (Riviera Beach, FL, USA). The dn/dc values were: polyMHist: 0.190 ml/g, co-1: 0.175 ml/g, co-2: 0.177 ml/g, co-3: 0.182 ml/g. Proton NMR spectra of the monomer and the polymers were recorded in D_2O on a 400 MHz spectrometer (JEOL EX400, Japan). The FT-infrared spectra of the same compounds were recorded on a FTS 6000 Biorad spectrophotometer. The MALDI-TOF mass spectra were recorded in the reflection mode, using a Voyager-DE STR instrument (Perseptive Biosystem) mass spectrometer, equipped with a nitrogen laser (λ = 337 nm, pulse width = 3 ns), working in a positive ion mode. The accelerating voltage was 25 kV, the grid voltage and the delay time (delayed extraction, time lag) were optimized for each sample to achieve the higher mass resolution (FWHM). The laser irradiance was maintained slightly above threshold. The samples used for the MALDI analyses were prepared as follows: 10 µl of polymer solution (10 mg/ml in H_2O or C_2H_5OH) were mixed with 30 µl of HABA solution (0.1M in C_2H_5OH), then 1 µl of each analyte/matrix mixture was spotted on the MALDI sample holder and slowly dried to allow the analyte/matrix co-crystallization. A mass resolution of about 4000 Da was obtained in the best MALDI mass spectra recorded.

2.4. Viscometric measurements

Viscometric measurements were carried out with an AVS 310 automatic Schott-Gerate viscometer at 25°C on a dilute aqueous polymer solution. The solution was freshly prepared by weighing and dissolving a known amount of the polymeric compound (MHist content, mmol: polyMHist, 0.2154; co-3, 0.2258; co-2, 0.2258; co-1, 0.1368) in 25 ml of 0.15M NaCl containing a measured volume of standard 0.1M NaOH solution. A standard 0.1M HCl solution was stepwise delivered by a Metrohm Multidosimat piston buret. The evaluation of the pH, at each neutralization step, was made with the program Fith [27] from the $\log K^{\circ}$ and the n values of the corresponding polymer and copolymers (see basicity constants, section 3.2). Viscometric data at different temperatures were obtained on polymer solutions at three different significant pHs (9, 5, and 2). A weighed amount of copolymer (co-1, 336 mg; co-2, 282 mg; co-3, 97.9 mg) was dissolved in 25 ml of 0.15M NaCl and the pH was controlled by adding the stoichiometric quantity of standard NaOH or HCl solutions. The temperature was monitored by the Haake DC10 thermostat (Thermo Electr. Corp.).

2.5. Potentiometric measurements

The acid-base potentiometric measurements were carried out in aqueous media at 25°C, following a previously reported procedure [6, 19]. A TitraLab 90 titration system (from Radiometer Analytical), consisting of three components (Titration Manager, TIM900; high-precision autoburet, ABU901; and the sample stand) and connected to the TimTalk 9 (a Windows based software, for remote control) was used to record the potentiometric titration data of the monomer, the polymers, and the hydrogel. All the titrations were carried out in a thermostated glass cell filled with 100 ml of 0.15M NaCl in which a weighed quantity of solid material and a measured volume of standard HCl solution were dispersed by magnetic stirring, under a presaturated nitrogen stream. Forward titrations were carried out with a standard 0.1M NaOH solution and reliable results were obtained for the back-titration with a standard 0.1M HCl solution. Unlike the monomer and the polymers, which, being soluble over the whole pH-range investigated were titrated at the equilibration time of 300 s for each titration step (0.04 ml), the MH2 roughly and finely crushed hydrogel sample (0.1205 mmol) was titrated at different equilibration times (1500 and 3000 s). In the case of the roughly crushed hydrogel, hysteresis loops were obtained during the forward and backward titrations with NaOH and HCl standard solutions, respectively; the finely crushed hydrogel improved a faster response in reaching equilibrium conditions. A typical potentiometric titration curve for the soluble compounds is reported in Figure 2,

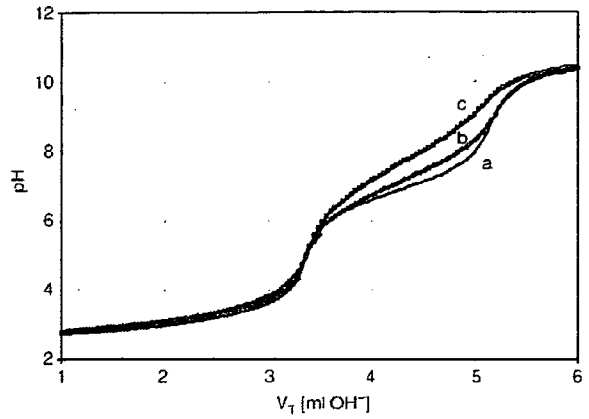

Figure 2. Potentiometric titration curves (pH in relation to the volume of standard NaOH 0.1084M) of MHist (a, 0.1997 mmol), co-3 (b, 0.2090 mmol), and polyMHist (c, 0.1864 mmol) in 0.15M NaCl at 25°C

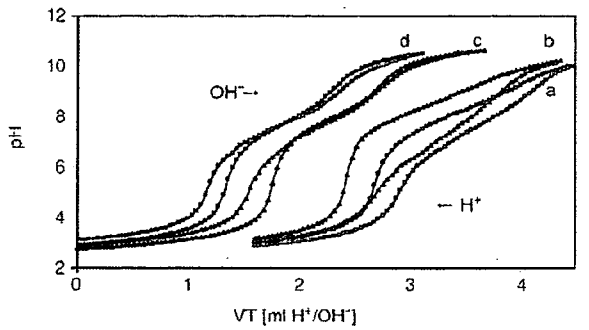

Figure 3. Potentiometric titration curves of the MH2 hydrogel (a, b: roughly crushed; c, d: finely crushed) protonation in 0.15M NaCl at 25°C. Equilibration time for each titrant addition (0.04 ml of 0.1205M NaOH forward, blue curves; 0.04 ml 0.1123M HCl backward, red curves): 1500 s (triangle) and 3000 s (square)

while Figure 3 shows the titration curves of the MH2 hydrogel in the rough and fine crushing state. The basicity constant (log*K*) values of the monomer were evaluated with the Superquad program [28] taking into account all the points of three independent potentiometric titration curves (ca. 300 data points) carried out with a different amount of ligand (0.13–0.20 mmol). On the other hand, the basicity constants of the free (polyMHist, 0.15–0.19 mmol; co-3, 0.21 mmol; co-2, 0.23 mmol; co-1, 0.13 mmol) and the cross-linked polymers (MH2, 0.12–0.15 mmol) were evaluated with the ApparK program [27]. In these cases each potentiometric titration was computed to evaluate both the log*K*s into a separated pH-buffered region. In all cases, the $E°$ calibrations were performed before and after each titration with the standard Tris grade-reagent. Three replicates were averaged and their standard deviations calculated.

2.6. Calorimetric measurements

Calorimetric measurements were carried out in aqueous solution at 25°C, following a previously reported procedure [6], by the use of a Tronac titration calorimeter (mod 1250) operating in the isothermal mode. A stainless steel reaction vessel was filled with 25 ml of 0.15M NaCl (containing a measured amount of standard NaOH solution) in which a weighed quantity of solid material (MHist content, mmol: monomer MHist, 0.12–0.24; polyMHist, 0.14–0.22; co-3, 0.13–0.23; co-2, 0.13–0.23; co-1, 0.14) was dissolved and titrated with a standard 0.1M hydrochloric acid solution at a BDR (buret delivery rate) of 0.0837 ml/min through a Gilmont buret. The titrations were performed at high and low MHist content for the protonation of the only imidazole nitrogen and for the protonation of both the imidazole and the carboxylate groups, respectively. Before and after each experiment, the chemical calibration with Tris/HCl and the corrections for the heats of the titrant dilution were made. All the experiments were automatically controlled by the Thermal program (from Tronac, Inc.) which was renewed to operate through a NI-DAQ driver software in Windows (from National Instruments). The graphical programming language LabVIEW was used to create the application. The evaluation of the enthalpy change ($-\Delta H°$) values was obtained with the Fith program [27] by taking into account the linear dependence of the log*K*s on α (the degree of protonation) for the polymeric compounds. The entropy change ($\Delta S°$) values were calculated. The results of at least two replicates were averaged.

2.7. Swelling measurements

Swelling measurements of the hydrogels (MH2 and CMH2) were carried out in different conditions of pH and temperature, at equilibrium conditions. The equilibrium degree of swelling (EDS) was measured every 24 h because the kinetic DS/time curves reached a plateau in these conditions. A weighed sample of dry gel (MH2, 30.4 mg; CMH2, 28.7 mg), contained in a Strainer cell (100 μm pore size), was immersed in a thermostated glass cell filled with

100 ml of aqueous solution at the desired pH, under stirring by the magnetic bar. The temperature probe and the pH glass electrode were controlled by the TimTalk 9 software. The EDS in relation to pH for both the hydrogels was monitored at different pHs of the proper buffer. The EDS in relation to the sodium chloride concentration was monitored at 25°C and in Tris/HCl buffered solution at pH 9.02 by the daily addition of weighed portions of the salt to produce the desired final concentration. The effect of the temperature for the CMH2 gel was monitored in buffered solutions at three different pHs (9.02, 5.01, and 3.07) and at a constant ionic strength (0.15M NaCl). In all cases, the gel sample and its container were removed from the bath at intervals, blotted with a tissue paper to remove any surface droplets, and weighed (wet weight, W_{wet}). The procedure was repeated at 12–24 h intervals. The EDS value was calculated by the relation: EDS = $(W_{wet}-W_{dry})/W_{dry}$, where W_{dry} is the weight of the dry gel sample.

2.8. Electric measurements

Hydrogels contraction measurements were carried out at 25°C according to the previously reported procedure [19]. A constant voltage was applied between two gold electrodes (16 mm diameter) in a cylindrical nylon cell, and with a mobile cathode positioned on the gel sample. The hydrogels (CMH2 and CMH10) were swollen in a 0.01M Tris/HCl buffer solution at pH 9, then a specimen of 5 mm thick was cut and used for contractile experiments for a period of 10 min. Under the application of the electric field, each hydrogel change in the thickness was controlled by a digital comparator that was sensitive to displacements of 10^{-2} mm (Digimatic indicator 266-2745, Mitutoyo). All the experiments were controlled through a NI-DAQ driver software in Windows (from National Instruments) and the graphical programming language LabView was used to create the application. The gel deformation was recorded at intervals of 1 s under the applied voltage (2.5, 5.0, and 7.0 V) by a dc power supply.

2.9. Evaluation of cytotoxicity

Cell culture

Mouse osteoblast cells (MC3T3-E1) obtained from the RIKEN Cell Bank (Tsukuba, Ibaraki, Japan) were cultured to confluence in culture dishes (Corning *Co., Ltd.*) containing a medium composed of Minimum Essential Medium, alpha modified (MEM-α, Kohjin Bio *Co. Ltd.*, Japan) supplemented with 10% fetal bovine serum (FBS,BioWest, France) in a fully humidified atmosphere with a volume fraction of 5% CO_2 at 37°C.

Cytotoxicity evaluation

The cell viability was evaluated by using a Cell Counting Kit [29] (WST-1 method, Dojindo Lab., Tokyo, Japan). Briefly, after the MC3T3-E1 cells reached confluency, they were trypsinized and seeded at $1 \cdot 10^4$ cells/cm^2 onto 96-well multiplate (Corning *Co., Ltd.*) then incubated for 2 days in a humidified atmosphere containing 5% CO_2 at 37°C. After removing the cultured medium, 100 µl of fresh culture medium supplemented with 10% [v/v] FBS and containing each MHist sample were added to each well and allowed to stand for in a fully humidified atmosphere with a volume fraction of 5% CO_2 at 37°C. After 24 h of incubation, 10 µl of WST-1 reagent were added to each well and the wells incubated for 2 h at 37°C; then 10 µl of 0.1N HCl aqueous solution were added to each well to stop the reaction. The absorbance of aliquot of the solution was measured at 450 nm, with a reference of the absorbance at 655 nm, with a multiplate reader (Bio-Rad model 650, Tokyo, Japan). The results were expressed as viability [%] related to a control containing no MHist samples. The error bar means standard error of four experiments.

3. Results and discussion

3.1. Syntheses and characterization

Monomer

The *N*-methacryloyl-L-histidine (MHist) was prepared according to the synthetic route to obtain vinyl monomers from α-aminoacids [2, 4–6, 22–24]. The reaction between methacryloyl chloride and L-histidine at low temperature (< 5°C) allowed to obtain a white powder freely soluble in water. The

Table 1. Main IR frequencies [cm^{-1}] and protonNMR chemical shifts (δ [ppm]) of *N*-methacryloyl-L-histidine

	Assignments
IR	1709 (*w*) C=O stretch of COOH group; 1656 (*s*) Amide I; 1620 (*sh*) C=C; 1600 (*vs*) Imidazole group; 1534 (*s*) Amide II; 1437 (*w*) $-CH_3$; 1393 (*vs*) C=O stretch of COO^- *w*: weak; *s*: strong; *sh*: shoulder; *vs*: very strong
^{1}H NMR	1.75 (s, 3H $CH_3C(=CH_2)H-$); 2.95–3.23 (m, 2H –CH2– Imidazole); 4.41–4.46 (q, H $-NHCH(COOH)CH_2-$); 5.31–5.52 (m, 2H $CH_2=C(CH_3)-$); 7.12 (s, 1H Imidazole, –C=CHN=); 8.44 (s, 1H Imidazole, –N=CHNH–)

potentiometric purity revealed that the imidazole nitrogen was protonated more than 92 wt%, while the carboxyl group was mostly in the ionized form. The expected structure was confirmed by the ^{1}H NMR and FT-IR spectroscopy. Table 1 summarizes the observed main infrared frequencies and the chemical shifts of the MHist.

Unlike the previously reported acrylate monomer, the *N*-acryloyl-L-histidine (Hist), the MHist showed the presence of a great amount of amphoteric molecular species [6]. The lower chemical shifts of the imidazole protons and the very strong band at 1600 cm^{-1} are indicative of the prevailing zwitterionic molecules [19]. This is also supported by the greater basicity constant.

Polymers

The *N*-methacryloyl-L-histidine, MHist, was used as the starting pH-sensitive monomer to synthesize free and cross-linked polymers together with the thermoresponsive *N*-isopropylacrylamide, NIPAAm, by a radical polymerization [4–6]. Unlike the poly(*N*-methacryloyl-L-histidine), the polyMHist, that was obtained in ethanol and using the AIBN initiator, the three copolymers with NIPAAm (co-3, co-2, and co-1), along with the three hydrogels (MH2, CMH2, and CMH10), were obtained in water solution by the use of the APS initiator [19–26]. While the free polymers remained in solution during the polymerization process, the cross-linked compounds gelified within 4 hrs. Compared to the acrylate analogue [6, 19], the polymerization of the methacrylate MHist to the corresponding

Table 2. Results of molecular characterization of polyMHist homopolymer and copolymers by SEC-MALS

Sample	MHist content [weight%]	dn/dc [ml/g]	M_p [kg/mol]	M_w [kg/mol]	M_w/M_n
PolyMHist	96.5	0.190	81.4	83.2	3.2
co-1	9.1	0.175	481.3	–	–
co-2	17.9	0.177	792.2	831.6	2.0
co-3	51.5	0.182	304.0	380.0	2.2

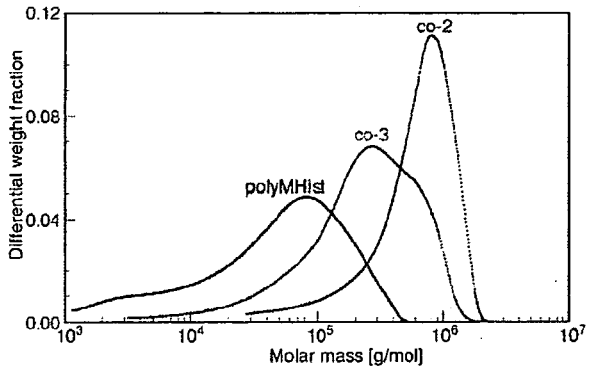

Figure 4. Comparison of the differential molar mass distribution of polyMHist homopolymer, co-2 and co-3 copolymers by SEC-MALS

homopolymer gave rise to a relatively lower number-average molecular weight, while the polydispersity index remained quite high, even after the dialysis process (Table 2).

This may be ascribed to the different solvent used in the polymerization procedure [25]. Figure 4 shows the comparison of the differential molar mass distribution (DMM) of the polyMHist homopolymer and the two copolymers (co-2 and co-3) bz SEC-MALS.

Unfortunately, the chromatographic elution of the copolymers depends on the NIPAAm content. In particular, Figure 4 does not report the DMM of co-1 copolymer because the chromatogram presents a long tail in consequence of a very high NIPAAm content (about 90%). Consequently, for the co-1 copolymer Table 2 reports only the peak molar mass M_p. It is important to note that the molar mass values from MALS are absolute and do not depend on an eventual non-steric chromatographic elution. As a result the M_w and M_p molar mass values are substantially correct, while the polydispersity index M_w/M_n (see Table 2) and in general the DMM shape (see Figure 4) are only approximate.

Table 3. Molar composition of vinyl polymers containing L-histidine residues

Compd	MHist purity, [mol%]	
	Potentiometry	Proton NMR
PolyMHist	96.5	100.0
co-3	35.0	36.5
co-2	10.0	8.2
co-1	4.9	3.5

The copolymers with NIPAAm produced higher molecular weight compounds that in general increased with the NIPAAm content. This led also to a greater viscosity in a wide range of pH (see the protonation section). However, in all cases the ^{1}H NMR spectra showed that the chemical shifts of the vinyl double bond (5.31–5.52 ppm) completely disappeared, and the broad lines were consistent with the presence of a slowly tumbling macromolecular species in D_2O solution. The FT-IR spectra confirmed the total conversion of the monomers into the corresponding polymers. The band intensity at 1599 cm^{-1} present in the polyMHist decreased as the NIPAAm unit increased in the copolymers. In the meantime, the new band of the NIPAAm Amide I increased and slightly shifted to greater wavenumbers, in the same way as happened for the 1459 cm^{-1} band of the isopropyl group [31, 32].

Based on the NMR and potentiometric results, the relative comonomer MHist/NIPAAm incorporation level reflected the comonomer feed ratio. Table 3 shows that the amount [mol%] of titrated MHist in the polymers is in agreement with that evaluated by the proton signals of the methyl groups.

These results suggest a presumably total conversion of the monomers into the corresponding polymers, being the reaction of radical type. A random distribution of MHist units in copolymers with NIPAAm may be expected because the basicity constants and the n values showed a decreasing trend (see protonation section). When both the monomers had a close structure, a random distribution of charged units was observed in the copolymer. This reflects lower electrostatic effects due to a lower content of charged groups. [25, 30, 32]. Moreover, the hydrogels were obtained at the fixed amount of cross-linking agent (EBA, 2 and 10 mol%) and with a NIPAAm/MHist molar ratio of 0 and 12, in order to have, respectively, a greater content of pH- or temperature-responsive comonomer content. After the polymerization procedure, the samples were slowly dried at r.t. for a week and then under vacuum. As expected, the acid/base potentiometric titrations of the gel MH2 revealed that the imidazole nitrogen content of

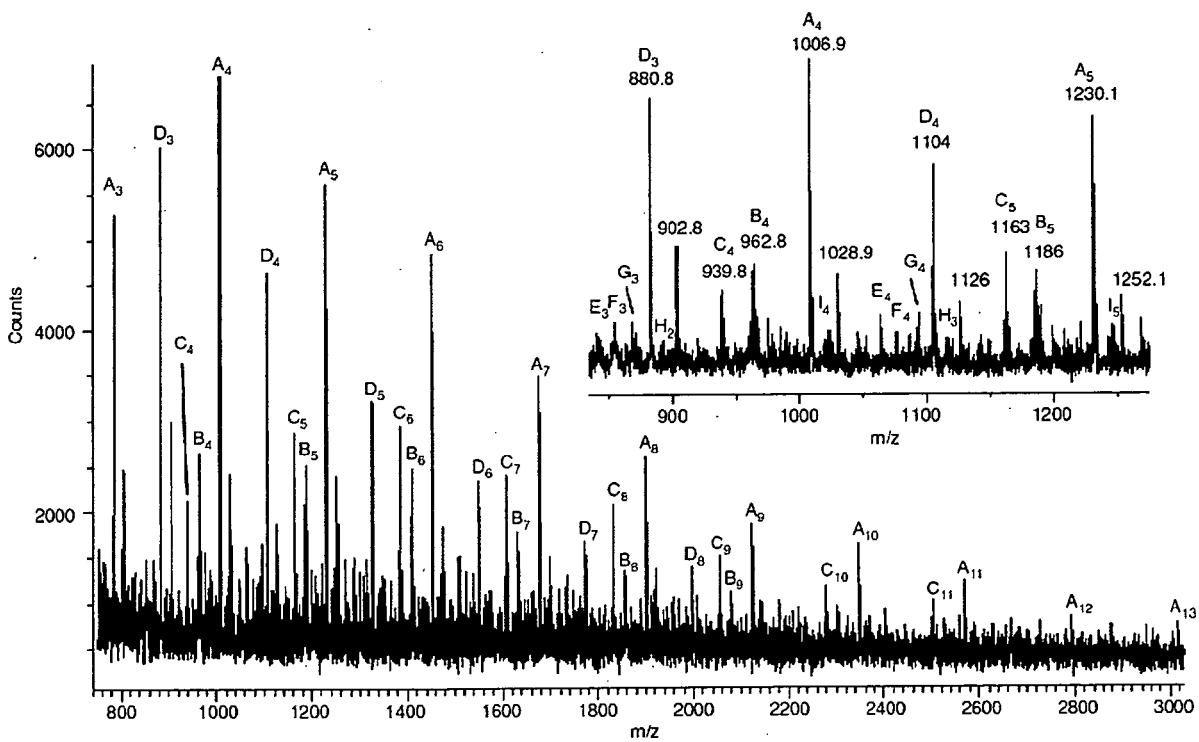

Figure 5. Positive ions MALDI-TOF mass spectrum of the polyMHist sample

Table 4. Structural assignments of peaks displayed in the MALDI-TOF mass spectrum of the polyMHist

Structures[a]	$[MH]^+$ (n)[b]	$[M+Na]^+$ (n)[b]
A= 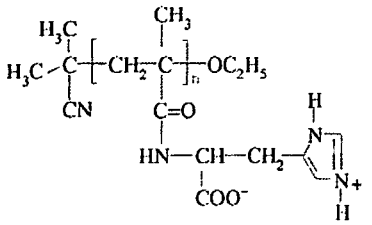	783.7 (3) 1006.9 (4) 1230.1 (5) 1453.3 (6) 1676.5 (7) 1899.7 (8) 2122.9 (9) 2346.1 (10) 2569.3 (11) 2792.5 (12) 3015.7 (13)	805.7 (3) 1028.9 (4) 1252.1 (5) 1475.3 (6) 1698.5 (7) 1921.7 (8) 2144.9 (9) 2368.1 (10) 2591.3 (11) 2814.5 (12) 3037.7 (13)
B= 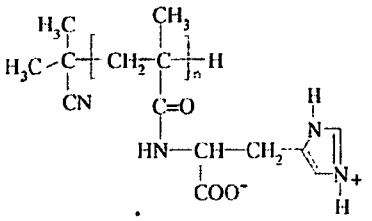	962.8 (4) 1186.0 (5) 1409.2 (6) 1632.4 (7) 1855.6 (8) 2078.8 (9) 2302.0 (10) 2525.2 (11) 2748.4 (12) 2971.6 (13)	984.8 (4) 1208.0 (5) 1431.2 (6) 1654.4 (7) 1877.6 (8) 2100.8 (9) 2324.0 (10) 2547.2 (11)
C= 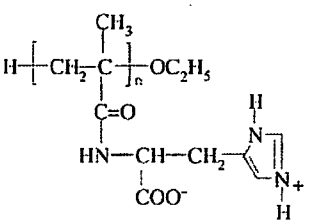	939.8 (4) 1163.0 (5) 1386.2 (6) 1609.4 (7) 1832.6 (8) 2055.8 (9) 2279.0 (10) 2502.2 (11) 2725.4 (12) 2948.6 (13)	961.8 (4) 1185.0 (5) 1408.2 (6) 1631.4 (7) 1854.6 (8) 2077.8 (9) 2301.0 (10) 2524.2 (11) 2747.4 (12) 2970.6 (13)
D= 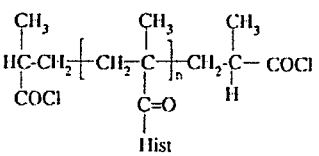	880.8 (3) 1104.0 (4) 1327.2 (5) 1550.4 (6) 1773.6 (7) 1996.8 (8)	902.8 (3) 1126.0 (4)
E= 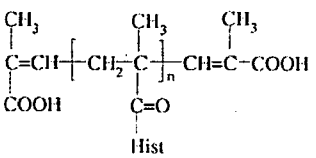	840.6 (3) 1063.8 (4)	
F= 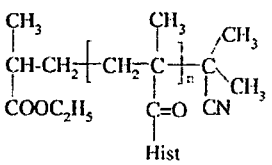	853.6 (3) 1076.8 (4)	
G= 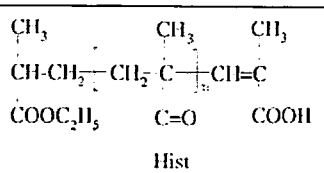	870.6 (3) 1093.8 (4)	

Table 4. Continued

Structures[a]	$[MH]^+$ (n)[b]	$[M+Na]^+$ (n)[b]
H= 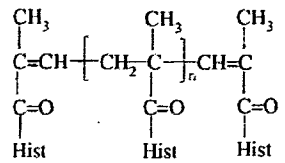	893.8 (2) 1117.0 (3)	
I= 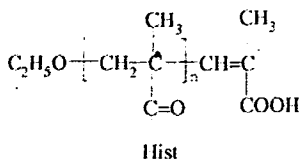	1023.8 (4) 1247.0 (5)	

a) Hist = 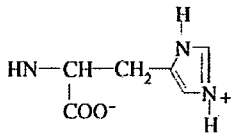

b) Values in parentheses are the repeating units

MHist was in agreement with the feed composition. The potentiometric curves showed large hysteresis loops [4] during the forward and backward titrations with NaOH and HCl solutions, respectively (Figure 3). This may be ascribed to the grinded state of the sample, considering that the MH2 gel particles were large and compact. The large size distribution of the material, along with its compactness, may slow down the equilibration for the protonation mechanism of the gel MH2, due to a hard deep diffusion of the hydrated H^+/OH^- ions into the interior of the gel particles. The potentiometric curves reached a faster equilibrium condition when a finely crushed sample of MH2 was titrated at the equilibration time of 1500 s and 3000 s for each titrant (H^+/OH^-) addition (Figure 3).

The MALDI-TOF mass spectrometry technique [33–35] has been used to characterize the chemical structures of the polyMHist oligomer components. Figure 5 reports a typical mass spectrum of the polyMHist, recorded in reflection mode, using HABA (0.1N in C_2H_5OH) as a matrix and the polymer dissolved in water. This spectrum exhibits a series of peaks from 750 up to 3000 Da corresponding to the protonated and sodiated ions of the polyMHist oligomers with a variety of the end groups, and they have been assigned (Table 4) to a specific oligomer structure. The identification of the structure and the end groups attached to the oligomers produced in the free-radical polymerization process is of utmost importance, since the end groups reveal the particular mechanisms that have been active in the polymerization process. The structures of the oligomers corresponding to the mass peak series A, and B in Figure 5, belonging to the expected oligomers terminated with isobutironitrile (IBN) groups at one end (Table 4), are due to the initial reaction of the radical initiator with the monomer MHist. The oligomers A are also terminated with an etoxyl group ($-OC_2H_5$) at the other end chain, indicating that a reaction between macroradicals and the ethanol used as solvent occurred. The oligomers B, besides the IBN groups, are terminated with H and are maybe generated by a H-extraction reaction, that occurs in a typical free-radical polymerization. The last two reactions led to the oligomers C which are terminated with –H and $-OC_2H_5$ species (Table 4). The intense peaks belonging to the mass series D were assigned to the unexpected oligomers terminated with methacryloyl chloride groups at both the ends. These are due to the metacryloyl chloride unit present as not detectable trace in the purified MHist used as monomer in the synthesis of the polyMHist sample. These peaks disappeared when the crude polyMHist sample was dissolved in ethanol to prepare the sample for the MALDI analysis, giving in this case intense mass peaks due to the corresponding oligomers with ethyl methacrylate end chains. Looking at the inset in Figure 5, we observe the

presence of weak mass peaks labelled as E, F, G and I (Table 4) corresponding to the oligomers that could be generated from oligomers terminated with metacryloyl chloride groups. Finally, the oligomers species indicated as H and I, as well as the species G, bearing unsaturated end groups (see Table 4) could be formed by the disproportionation reactions that occur during the conventional free radical polymerization.

3.2. Protonation study

Potentiometry, viscometry, and solution calorimetry were the main techniques used to study the protonation behaviour of the monomer, the polymer, the copolymers and the hydrogels at 25°C in aqueous 0.15M NaCl.

Basicity Constants and viscometry

The basicity constant values for the protonation of the basic imidazole nitrogen ($\log K_1$) and the carboxylate group ($\log K_2$) in the MHist and in the related polymer and copolymers are reported in Table 5. In the same table the basicity constants for the MH2 hydrogel is also reported.

The presence of the methyl groups in the main chain of the polymer structure strongly reduces the polyelectrolyte behaviour because of the increased hydrophobicity. The $\log K_1$ of the MHist (6.88) showed a greater value than that of the Hist (6.48) for inductive effects. On the other hand, the corresponding polymeric compound showed a quite similar $\log K$ value. The hydrogel MH2 showed greater $\log K$s and a lower n value; this trend, being similar to the previously studied acrylate hydrogels, may be attributed to the reduced conformational freedom because of the cross-linked network structure.

However, in all cases the $\log K$s follow the modified Henderson-Hasselbalch equation [36] showing a linear decreasing pattern on the degree of protonation α of the whole macromolecule. The experimental data, i.e. pH in relation to α, fitted very well the generalized Henderson-Hasselbalch equation (1):

$$pH = \log K_i^\circ + n \cdot \log[(1 - \alpha)/\alpha] \quad (1)$$

which has been checked experimentally for a number of polyelectrolytes [37, 38]. The linear relationship between pH and $\log[(1 - \alpha)/\alpha]$, over a wide range of α values, gives a straight line for all the compounds studied (Figure 6).

This led to exclude any transition region between the coil to compact structure, as occurred for other class of polyelectrolytes [37, 38]. The n value for the protonation of the imidazole nitrogen in the polyMHist and the corresponding copolymers, being related to the magnitude of the electrostatic interactions as well as being a measure of the hydrophilic influence [39], is always much lower than that reported for the acrylate analogue. Fur-

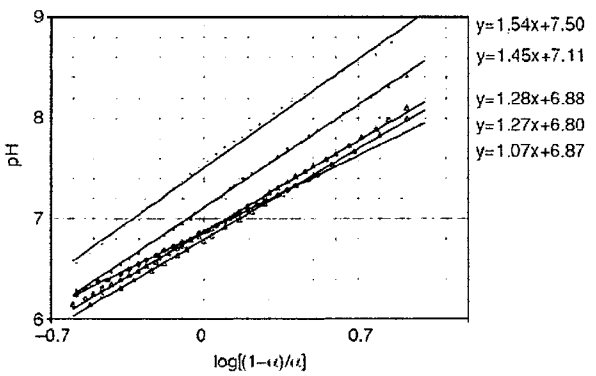

Figure 6. Typical Henderson-Hasselbalch plots of the MHist soluble compounds in 0.15M NaCl at 25°C

Table 5. Basicity constants of vinyl compounds containing L-histidine residues at 25°C in 0.15M NaCl

Compd	$\log K^\circ_1$	n_1	$\log K^\circ_2$
MHist	6.878 (2)		2.772 (6)
Hist[a]	6.48		–
PolyMHist	7.53 (7)	1.49 (5)	2.0
MH2	7.66 (18)	1.29 (9)	2.5
PolyHist[a]	7.64	2.22	2.3
co-3	7.06 (6)	1.41 (6)	2.5
co-2	6.84 (6)	1.23 (7)	2.8
co-1	6.70 (12)	1.15 (12)	2.8
Poly(Hist-*co*-NIPAAm)[a]	7.11	1.76	2.9
	$\log K_1 = \log K^\circ_1 + (n_1 - 1)\log[(1 - \alpha)/\alpha]$		

[a]Values in parentheses are standard deviations. Ref. 6.

thermore, as the protonation of the imidazole nitrogen is concerned, the linear decreasing pattern of the logK_1, and also of the n_1, in relation to the MHist content in copolymers with NIPAAm, is a result of the increased distance between the charges along the chain. This reduces the electrostatic contribution of the charges and shows as the monomers are randomly distributed with a predominance of block-like NIPAAm units. Similar results were previously reported for vinyl related copolymers containing L-valine residues [30, 31]. In the latter case, the decreasing trend of the log$K$ for the acrylates was ascribed to the increased distance between the charges, while methacrylate compounds showed a closer homopolymer polyelectrolyte behaviour. A block-like distribution of the charged methacrylic units was hypothesized in view of their different monomeric structures. In the case of the poly (ampholyte)s, any increase of the uncharged NIPAAm units, leads to a decrease of the proton up-take by the basic imidazole nitrogen. The logK_1 decrease is always due to the lower decreased electrostaticity exerted by the charged carboxylate anions. When the MHist content is very low, the logK_1 value approaches that of the corresponding monomer. On the other hand, the protonation of the carboxylate group in the copolymers cannot be well depicted because of the low basicity constants. These values account only for a limited degree of protonation in the experimental condition of this study.

The viscometric data well support the protonation-like mechanism of the polymers containing MHist. Figure 7 shows the reduced viscosity pattern at different pHs of the homopolymer polyMHist, while Figure 8 shows the conformational behaviour of the corresponding three copolymers.

In all cases, the fully ionized macromolecule (L^-) is in the extended chain conformation. As the protonation of the basic imidazole nitrogen occurs, the coiling is sharp at pH close to the logK_1 and becomes the lowest at the maximum formation of the zwitterionic $L^{\pm}$ species. In the polyMHist, as the protonation proceeds, with the neutralization of the carboxylate anion, the coil dimension increases again for the presence of a net positive charge on the macromolecule (L^+). This trend, even if present in the copolymers co-3 and co-2, having relatively a greater amount of MHist content, was not shown in the copolymer co-1. Moreover, as the MHist

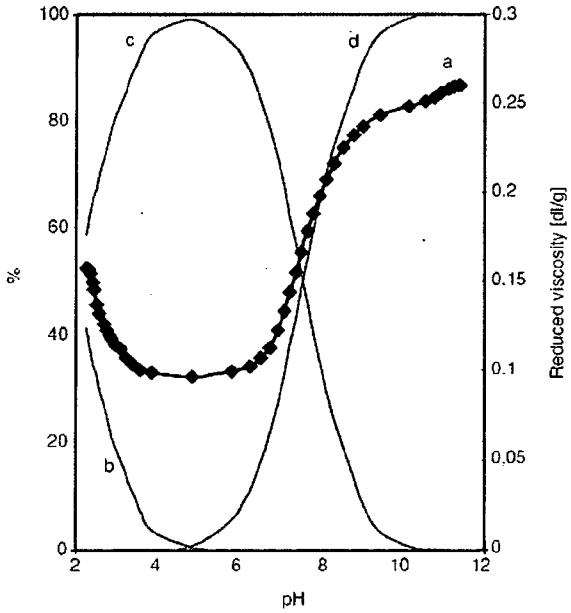

Figure 7. Reduced viscosity (η/C [dl/g]) of the polyMHist in relation to the pH (a) with the superimposed species distribution curves [%] obtained by the log$K$s evaluated at 25°C in 0.15M NaCl (b – di-protonated L^+; c – mono-protonated, zwitterionic $L^{\pm}$; d – un-protonated L^-, where L is the monomer unit of the polymer)

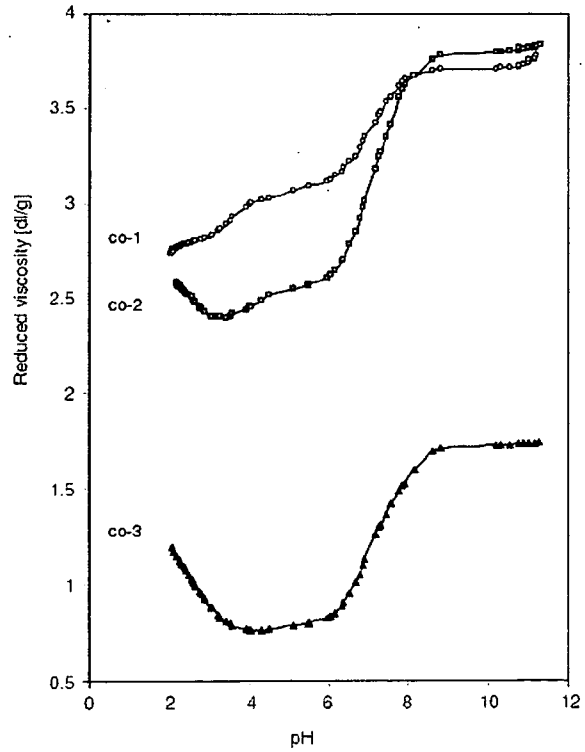

Figure 8. Reduced viscosity in relation to the pH for the poly(MHist-*co*-NIPAAm) copolymers at 25°C in 0.15M NaCl

content in the copolymers decreased, the lowest minimum of the reduced viscosity was shifted at lower pHs, with the disappearance in the *co*-1. Even if this behaviour seems to be quite interesting, the further collapse of the macromolecular coil at lower pH may be due to more competitive electrostatic-hydrophobic forces. During the protonation process, the polymer gradually uncoils, due to the increased electrostaticity of the protonated imidazole nitrogen. The hydrophobic forces between the isopropyl groups in NIPAAm are able to outweigh the repulsive electrostatic interactions when they are present at a critical concentration. A similar behaviour was already observed for vinyl poly (acid)s containing α-aminoacids with lateral isopropyl groups [30].

Enthalpy and entropy changes

The results of the calorimetric titrations revealed, for all the compounds considered, similar enthalpograms during the protonation of the basic groups present in the MHist moiety. The exothermic protonation reaction of the imidazole nitrogen revealed a well defined break-point corresponding to the amount of MHist close to that found by the potentiometry. The further protonation of the carboxylate anion showed a rather negligible endothermicity. Thus, we evaluated the enthalpy ($-\Delta H°$) and the entropy ($\Delta S°$) change values only for the imidazole nitrogen protonation (Table 6). The results of the methacrylate compounds (MHist and polymers containing MHist) showed rather similar protonation behaviour also when compared to the previously reported acrylate analogues [6].

Unlike the reported study on poly(Hist) [6], that showed a peculiar $-\Delta H°/\alpha$ plot and the protonation process of which was likely attributed to the formation of hydrogen bonds between adjacent monomer units, the poly(MHist) revealed a 'real' $-\Delta H°$ that was independent on the degree of protonation α. The different behaviour may be ascribed only to the presence of the further methyl group in the backbone macromolecular chain. Its hydrophobic character was evident in the greater $\Delta S°$ value of the MHist and the polyMHist when compared to the corresponding acrylate analogues [6]. However, the lower polyelectrolyte effect reported for the polyMHist during the protonation of the basic imidazole nitrogen is reflected in a lower $\Delta S°$ decrease on α, involving thus the release of further water molecules surrounding closer monomer units. In Figure 9 is reported the decreasing trend of $\Delta S°$ in relation to α for the protonation of the imidazole nitrogen in polyMHist and its copolymers with NIPAAm.

The trend is similar to that shown by the corresponding log*K*s, and, being the $-\Delta H°$ 'real' (i.e. independent on α), the polyelectrolyte effect is only attributed to entropy contributions. In fact, the protonation of the imidazole nitrogen led to a sharp decrease of the macromolecular coil with the for-

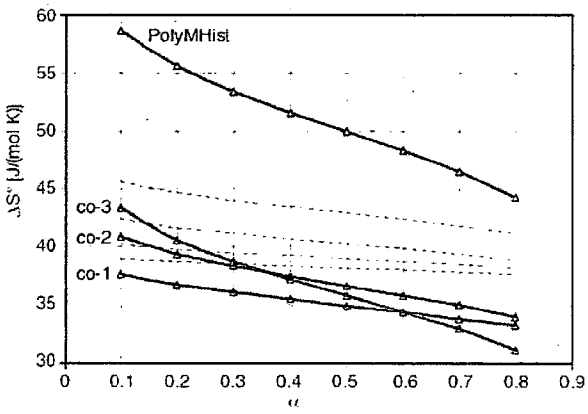

Figure 9. Entropy change ($\Delta S°$ [J/(mol·K)]) values in relation to α for the protonation of the imidazole nitrogen in polyMHist and related copolymers in 0.15M NaCl and 25°C. (Dotted lines refers to $-\Delta G°$ of the same compounds)

Table 6. Thermodynamic functions of the imidazole nitrogen protonation in vinyl compounds containing L-histidine residues (25°C in 0.15M NaCl)

Compd	$-\Delta G°$, [kJ/mol]	$-\Delta H°$, [kJ/mol]	$\Delta S°$, [J/(mol·K)]	Ref.
MHist	39.26 (1)	29.3 (2)	33.4 (7)	This work
Hist	37.0	30.5	21.8	[6]
PolyMHist	43.0 (4)	28.1 (4)	50 (1)	This work
PolyHist	43.6	30.6	44	[6]
co-3	40.3 (3)	29.6 (6)	36 (2)	This work
co-2	39.0 (3)	28.1 (6)	37 (2)	This work
co-1	38.2 (7)	28.7 (7)	35 (2)	This work
Poly(Hist-*co*-NIPAAm)	40.6	29.5	37	[6]

mation of zwitterionic species. Besides the likely ordering to some extend of the zwitterions, the process led to a release of water molecules because the macromolecule becomes tightly coiled. This was seen in some cases because phase separation occurred at the isoelectric point. As a matter of fact, the corresponding hydrogels decreased their degree of swelling for the loss of water molecules.

3.3. Swelling behaviour of hydrogels

The swelling behaviour of the hydrogels was studied in relation to the pH, the temperature, the electric current, and the concentration of the simple NaCl salt at pH 9, i.e. in the completely ionized form of the MHist units. The sample slabs swelling kinetics for the two different cross-linked CMH2 and CMH10 hydrogels was recorded at constant ionic strength (0.15M NaCl) and at two different pHs (1.9 and 8.8). The results, reported in Figure 10, show the different hydration ability in the different pH conditions. It is evident that the degree of swelling (DS) is greater for the less cross-linked CMH2 gel and at higher pHs. In both cases, the equilibrium DS was reached within few hours. Both the gels are friable in the dry state and become transparent as the water content increases.

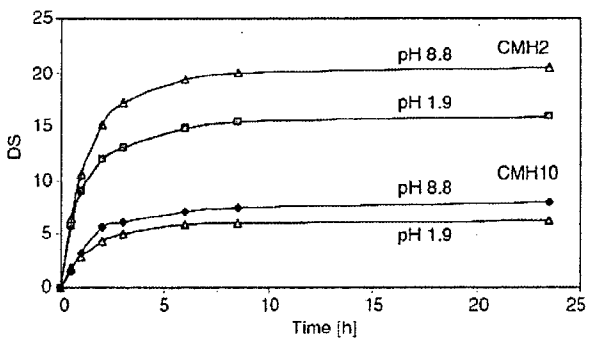

Figure 10. Swelling kinetics of the hydrogels CMH2 (slabs of 50 mg) and CMH10 (slabs of 55 mg) at two different pHs in 0.15M NaCl and 24°C

Effect of pH, temperature, ionic strength, and electric current

The swelling behaviour of the hydrogel MH2 in relation to pH, at 25°C in 0.15M NaCl, is reported in Figure 11. The EDS/pH plot, being similar to that reported for the viscometric data of polyMHist in Figure 7, sensitively reveals a decreasing pattern by increasing the pH in the narrow range 4 to 6. In

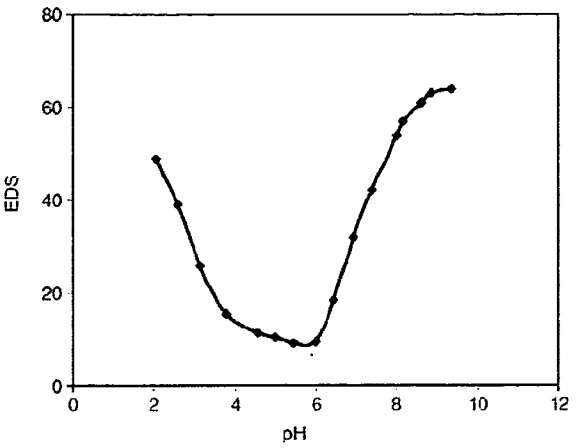

Figure 11. Equilibrium degree of swelling (EDS) in relation to the pH of the gel MH2 in 0.15M NaCl at 25°C

this pH-range the zwitterionic form predominates with its maximum at the isoelectric point (i.p., pH 5). It is likely that the greater log$K$ values of the hydrogel, with its lower polyelectrolyte behaviour, may lead to more stable ionized species of greater hydrophilic quality. As the pH shifts-out from this range, the gel MH2 swells as a consequence of its water content increase, due to the predominance of net positive or negative charges.

On the other hand, the hydrogel CMH2 behaves likewise the copolymer co-2, having the latter a similar comonomer composition. In Figure 12 the EDS/pH profile of the hydrogel CMH2 at 25°C in 0.15M NaCl is reported. Compared to the previously reported acrylate CH1 hydrogel containing Hist [19], the lower EDS value is due to the greater cross-link density in CMH2. The striking similarity of the swelling behaviour with the reduced viscos-

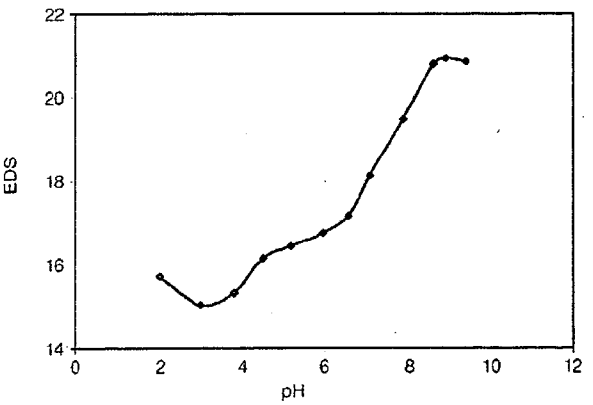

Figure 12. Equilibrium degree of swelling (EDS) in relation to the pH of the gel CMH2 in 0.15M NaCl at 25°C

ity (Figure 8) suggests a similar polyelectrolyte behaviour of the two polymers, even in the different free and cross-linked forms. On the basis of these results it is likely to hypothesize any tailoring hydrogel system to collapse at desired pHs, by introducing the right amount of the two co-monomers. Of course, if in these copolymers the MHist content becomes less than a critical value (about 5 mol%), the polyampholyte quality vanishes because of the superimposing effect of the hydrophobic interactions exerted by the isopropyl groups of the NIPAAm moieties.

As regards the effect of the temperature, Figure 13 shows the swelling behaviour of the CMH2 hydrogel in a wide range of temperatures. The hydrogel swelling was studied in 0.15M NaCl and in three different buffered solutions of significant pHs.

Any increase of the temperature resulted in a deswelling ability of the hydrogel. It retained its hydration state at high as well as at low pHs. Contrary to the previously reported acrylate hydrogel CH1 [19], the CMH2 hydrogel showed a phase separation at higher temperatures and at lower pHs. The presence of the hydrophobic MHist unit, instead of decreasing the LCST (Lower Critical Solution Temperature) [40] of the NIPAAm based hydrogels (32°C), revealed a greater temperature increase. This point will be better investigated even though the behaviour may be further on ascribed to the peculiar protonation mechanism of the MHist based hydrogels. A similar greater increase of the phase separation temperature was observed for the soluble copolymers. In Figure 14 is reported the relationship between the viscometric data and the temperature (in the range 25–46°C) of the three copolymers (co-1, co-2, and co-3) at the three significant pHs (9, most negatively ionized; 5, zwitterionic; 2, most positively ionized).

Unlike the straight line observed in all cases by co-3, the copolymer co-2 showed an increased negative line slope at pH 5, close to 38°C; on the other hand, the co-1 showed more negative line slopes at different temperatures, depending on the pH. Table 7 summarizes the obtained results. The observed differences are due to the different content of the MHist units in the copolymers; lower MHist content displayed greater responsiveness to pH and temperature. It is worthwhile noting the

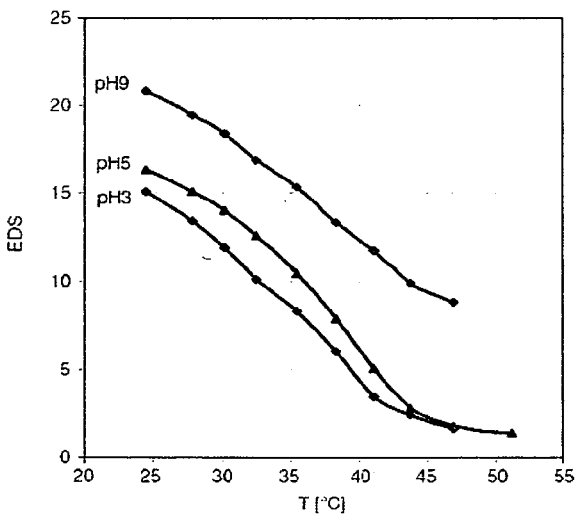

Figure 13. EDS of the gel CMH2 in relation to the temperature [°C] at three different pHs in 0.15M NaCl

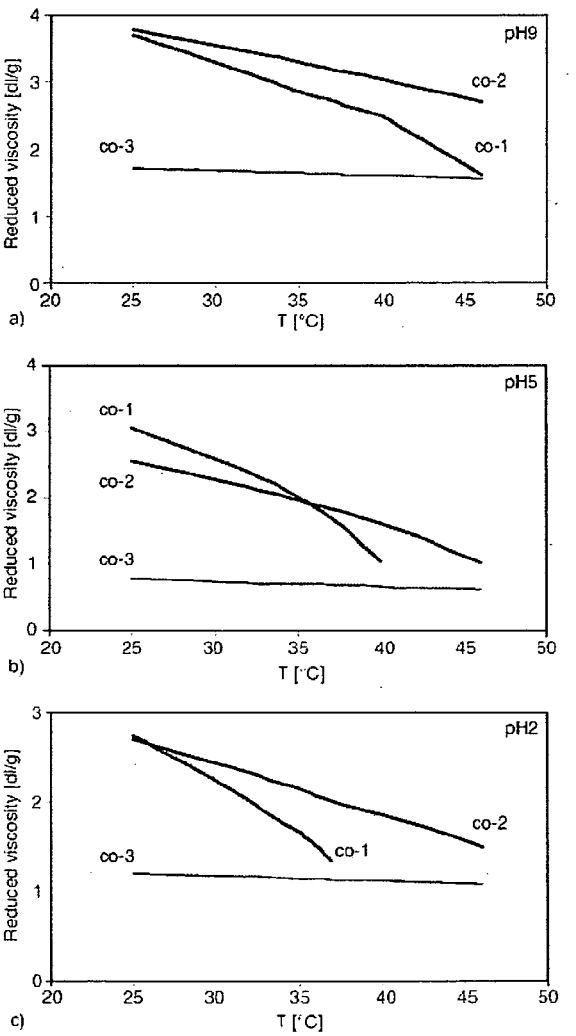

Figure 14. Reduced viscosity (η/C [dl/g]) of the three copolymers (co-1, red curves; co-2, green curves; co-3, blue curves) in relation to the temperature at three different pHs (9, 5 and 2) in 0.15M NaCl

Table 7. Straight line parameters from the reduced viscosity values of the three copolymers co-1, co-2, and co-3

Copolymer	pH	Line slope	R^2	Range of temperatures [°C]
co-3	2	–0.0054	0.990	25–46
	5	–0.0074	0.989	25–46
	9	–0.0079	0.995	25–46
co-2	2	–0.057	0.999	25–46
	5	–0.072	0.982	25–46
	5	–0.061	0.998	25–38
	5	–0.094	0.995	38–46
	9	–0.052	0.999	25–46
co-1	2	–0.115	0.994	25–46
	2	–0.109	0.998	25–35
	2	–0.166	0.993	35–37
	5	–0.126	0.964	25–46
	5	–0.105	0.996	25–35.5
	5	–0.205	0.997	35.5–46
	9	–0.096	0.981	25–46
	9	–0.083	0.999	25–40
	9	–0.146	0.999	40–46

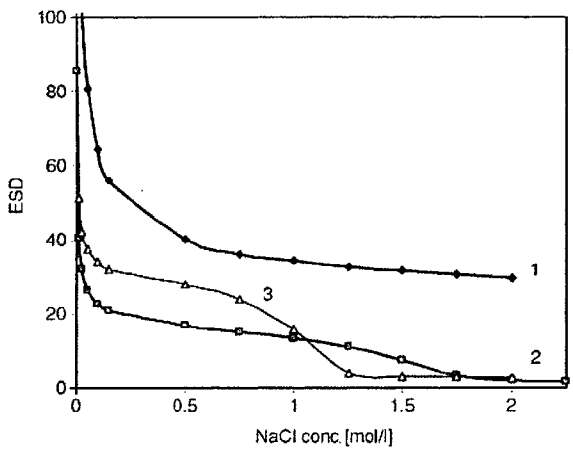

Figure 15. EDS of gels MH2 (1), CMH2 (2), and CH1 (3) [19] in relation to the concentration of NaCl (pH 9 and 25°C)

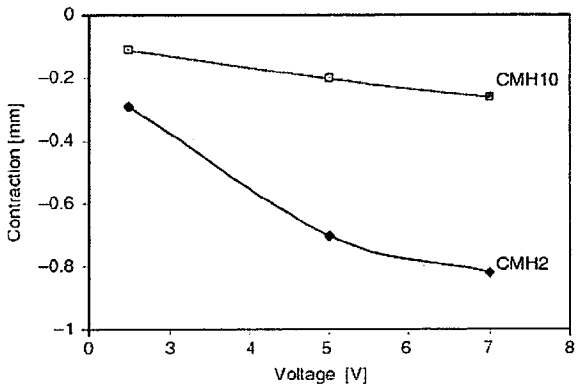

Figure 16. Hydrogel contraction [mm] in relation to the electric stimulation (2.5, 5.0, and 7.0 V) at 10 minutes elapsed time and pH 9

similar behaviour between the viscosity of the soluble co-1 and the EDS of the cross-linked gel CMH2 (Figure 13), having both the compounds similar MHist content. At the three different pHs, either the reduced viscosity and the EDS values follow the same trend and collapse almost at the same temperatures.

Moreover, the effect of the ionic strength, i.e. the concentration of sodium chloride, on the swelling properties of the MH2 and CMH2 hydrogels at pH 9, is reported in Figure 15 along with the results previously obtained with the gel CH1 [19], for comparison.

Unlike the hydrogel MH2, which shows only polyelectrolyte behaviour for the shielding effect of the carboxylate groups negative charges, the CMH2 showed a volume phase transition phenomenon at a NaCl concentration of 1.75 mol/l. This concentration resulted greater than that shown by the Hist-based CH1 hydrogel [19].

The electric current effect on the two hydrogels is reported in Figure 16. Any increase of the applied potential linearly increased the gel contraction. Moreover, the contraction of the gel CMH2 was higher than that of CMH10, because of the lower cross-links amount. These results, although more effective, are in agreement with the previously reported ones on the gels containing the acrylate Hist analogues.

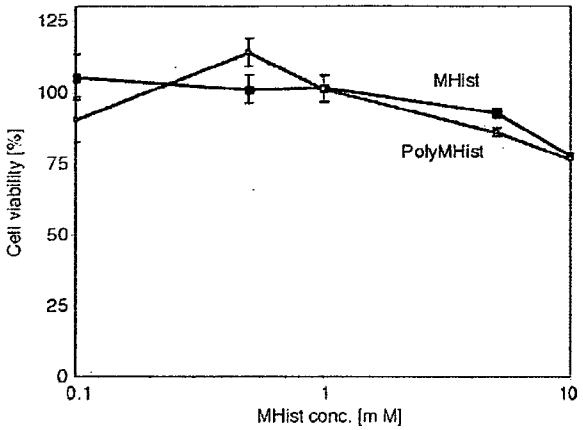

Figure 17. Cytotoxicity of the MHist and poly(MHist) against MC3T3-E1 (mouse osteoblast) cells

3.4. In vitro cytotoxicity

The cytotoxic effect of the poly(MHist) was evaluated by the cell culture of osteoblasts from mouse (MC3T3-E1). Figure 17 shows the cell proliferation in the presence of the polymer and its low-molecular weight precursor.

It is noticeable that no significant cytotoxicity was observed for two days at concentration up to 5 mM. Thus, these zwitterionic compounds in the cross-linked hydrogel form may show potential applications in bone resorption when implanted in specific tissues, for the releasing of loaded amino-bisphosphonate drugs [17].

4. Conclusions

This paper, concerning with our research interest on poly(ampholyte)s [6, 19, 41], developed a thermodynamic study for the protonation of basic groups in the free and cross-linked methacrylate polymers carrying the L-histidine residues. As a rule, methacrylate polyelectrolytes, particularly poly(carboxyl acid)s, show more complex thermodynamic data than the corresponding acrylates [42]. In the case of poly(ampholyte)s, the more hydrophobic character of the main polymer chain was evident in both the free and the cross-linked hydrogels. Unlike the corresponding acrylate, these new ligands show a lower polyelectrolyte behaviour. The 'real' enthalpy changes and the lower n values of the modified Henderson-Hasselbalch equation are the two main thermodynamic data showing the difference. Moreover, the volume phase transition behaviour of the hydrogels, based on the pH-responsive poly(ampholyte)s and on the temperature-responsive *N*-isopropylacrylamide, revealed that the thermodynamic data are close to the soluble analogues ones. The LCST of the polyNIPAAm, that is close to the body temperature, may be tuned by the pH and the proper amount of the purposely synthesized ampholyte monomer. Thermodynamic and biological characterization, along with the salt-induced phase transition and the dc electroshrinking phenomenon shown by the methacrylate hydrogels, are indicative of a suitability of these materials for tissue engineering applications [15]. The increasing hydrophobic character makes some poly(ampholyte)s suitable for the preparation of nonbiofouling surfaces against proteins and cells [22].

Acknowledgements

The research work was supported by a grant of the Italian MIUR, as a project within PRIN 2004, and by a grant of the PAR 2005 (Siena University). Thanks are due to Miss Ilaria Casolaro for having carefully read the manuscript.

References

[1] Casolaro M.: Stimuli-responsive polymers (thermodynamics in drug delivery technology). in 'Polymeric Materials Encyclopedia' (Ed.: Salamone J. C.), CRC Press, Boca Raton, vol. **10**, 7979–7992 (1996).

[2] Casolaro M., Paccagnini E., Mendichi R., Ito Y.: Stimuli-responsive polymers based on L-phenylalanine residues: the protonation thermodynamics of free polymers and cross-linked hydrogels. Macromolecules, **38**, 2460–2468 (2005).

[3] Barbucci R., Casolaro M., Magnani A.: Ionic and ionizable synthetic polymers: interactions in aqueous solution. Coordination Chemistry Reviews, **120**, 29–50 (1992).

[4] Casolaro M.: Thermodynamics of multiple-responsive polyelectrolytes with complexing ability towards the copper(II) ion. Reactive Polymers, **23**, 71–83 (1994).

[5] Bignotti F., Penco M., Sartore L., Peroni I., Mendichi R., Casolaro M., D'Amore A.: Synthesis, characterization and solution behaviour of intelligent polymers bearing L-leucine residues in the side chains. Polymer, **41**, 8247–8256 (2000).

[6] Casolaro M., Bottari S., Cappelli A., Mendichi R., Ito Y.: Vinyl polymers based on L-histidine residues. Part 1.: The thermodynamics of poly(ampholyte)s in the free and in the cross-linked gel form. Biomacromolecules, **5**, 1325–1332 (2004).

[7] Cho I., Shin J-S.: Hydrophobic and ionic interactions in the ester hydrolysis by imidazole-containing polymers. Bulletin of Korean Chemical Society, **3**, 34–36 (1982).